Human Molecular Genetics, 2012, Vol. 21, No. 5 **1049–1061**
doi:10.1093/hmg/ddr535
Advance Access published on November 16, 2011

Tuberin and PRAS40 are anti-apoptotic gatekeepers during early human amniotic fluid stem-cell differentiation

Christiane Fuchs, Margit Rosner, Helmut Dolznig, Mario Mikula, Nina Kramer and Markus Hengstschläger*

Institute of Medical Genetics, Medical University of Vienna, Währinger Strasse 10, Vienna 1090, Austria

Received September 12, 2011; Revised and Accepted November 13, 2011

Embryoid bodies (EBs) are three-dimensional multicellular aggregates allowing the *in vitro* investigation of stem-cell differentiation processes mimicking early embryogenesis. Human amniotic fluid stem (AFS) cells harbor high proliferation potential, do not raise the ethical issues of embryonic stem cells, have a lower risk for tumor development, do not need exogenic induction of pluripotency and are chromosomal stable. Starting from a single human AFS cell, EBs can be formed accompanied by the differentiation into cells of all three embryonic germ layers. Here, we report that siRNA-mediated knockdown of the endogenous tuberous sclerosis complex-2 (*TSC2*) gene product tuberin or of proline-rich Akt substrate of 40 kDa (PRAS40), the two major negative regulators of mammalian target of rapamycin (mTOR), leads to massive apoptotic cell death during EB development of human AFS cells without affecting the endodermal, mesodermal and ectodermal cell differentiation spectrum. Co-knockdown of endogenous mTOR demonstrated these effects to be mTOR-dependent. Our findings prove this enzyme cascade to be an essential anti-apoptotic gatekeeper of stem-cell differentiation during EB formation. These data allow new insights into the regulation of early stem-cell maintenance and differentiation and identify a new role of the tumor suppressor tuberin and the oncogenic protein PRAS40 with the relevance for a more detailed understanding of the pathogenesis of diseases associated with altered activities of these gene products.

INTRODUCTION

The description of Oct4-positive stem cells within human amniotic fluid (1) initiated a new and promising research field (2,3). Descending from a single-immunoselected CD117 (c-Kit)-positive human amniotic fluid stem (AFS) cell, lines can be established, which can be expanded as immature pluripotent stem cells able to differentiate along all three embryonic germ layers (4). These monoclonal AFS cell lines can be expanded in culture with high proliferative capacity, are chromosomal stable and do not need exogenic treatment to maintain pluripotency. Furthermore, AFS cells have a lower risk for tumor development and do not raise the ethical issues of embryonic stem (ES) cells. Accordingly, besides their putative functions in specific cell-based therapies, AFS cells became increasingly accepted as an ideal tool to study cell differentiation processes (2–5).

Pluripotent stem cells are also defined by their potential to spontaneously form three-dimensional multicellular aggregates called embryoid bodies (EBs). EBs allow the *in vitro* recapitulation and investigation of the three-dimensional and tissue level contexts of the cell differentiation phenomena during early mammalian embryogenesis (6,7). Recently, it was demonstrated that starting from one single human AFS cell, expressing the stem-cell markers CD117 and Oct4, EBs can be formed. When cultured in suspension, under conditions in which they are unable to attach to the surface of culture dishes, monoclonal AFS cells form EBs consisting of many different cells expressing ectodermal, endodermal and mesodermal markers (8). This *in vitro* recapitulation of the pluripotent AFS cell differentiation potential together with the recently established protocol for prolonged efficient siRNA-mediated gene silencing in human AFS cells (9) provides an optimal tool to study the relevance of specific

*To whom correspondence should be addressed. Tel: +43 14016056500; Fax: +43 140160956501; Email: markus.hengstschlaeger@meduniwien.ac.at

endogenous gene functions for early mammalian differentiation processes.

The serine/threonine protein kinase mammalian target of rapamycin (mTOR) is part of two distinct protein complexes in mammalian cells and is the central player within the insulin signaling pathway regulating cell size, tumor development and differentiation. The protein complex mTORC1, containing raptor and mLST8, phosphorylates the eukaryotic initiation factor 4EBP1 and the ribosomal p70S6 kinase (at T389 to activate the ribosomal protein S6), both being regulators of mRNA translation. mTORC2 contains rictor, mLST8, sin1 and protor, and phosphorylates the oncogenic kinase Akt at S473. Within the insulin signaling pathway, the phosphatidylinositol-3-kinase regulates the phosphoinositide-dependent kinase-1 to phosphorylate Akt at T308, what in conjunction with the above-mentioned mTORC2-mediated phosphorylation drives full activation of Akt. So, activated Akt stimulates mTORC1 activity via phosphorylating and thereby inhibiting the function of the two major negative regulators of mTORC1, the tuberous sclerosis complex-2 (*TSC2*) gene product tuberin and proline-rich Akt substrate of 40 kDa (PRAS40) (10–12).

Using siRNA-mediated endogenous gene silencing in human AFS cells during EB formation, we found tuberin and PRAS40 to be potent anti-apoptotic gatekeepers in early mammalian stem-cell differentiation. The discovery of this mTOR-dependent potential provides new insights into the development of tumors and human genetic diseases associated with functional loss of either tuberin or PRAS40.

RESULTS

Tuberin and PRAS40 regulate apoptosis during EB formation of AFS cells

siRNA-mediated knockdown of endogenous PRAS40 or tuberin triggered a pronounced degradation of EBs within several days of EB formation of human AFS cells (Fig. 1A and B). It is important to note that the used siRNA approach triggers gene knockdown for about 2 weeks in human AFS cells (9). Detailed microscopical investigation demonstrated significant morphological changes in the structures of the EBs. The inner area consists of cells with morphologies earlier described to be characteristic for AFS cell-derived EBs (8). Upon tuberin or PRAS40 knockdown, however, an outer area appeared consisting of less compacted, brighter shaped cells being typically described as the consequence of apoptotic processes (Fig. 1C) (13). Whereas the whole EB area remained unchanged (Fig. 1D), the inner diameter and the area of the EBs dramatically decreased upon PRAS40 or tuberin knockdown, accompanied by an increase in the surrounding outer ring and by decreased total cell number (Fig. 1E–G) in a time-dependent manner (Fig. 1H and I). These data demonstrate that tuberin and PRAS40 are essential gatekeepers inhibiting EB degradation during early human AFS cell differentiation.

Besides the detection of the already mentioned typical apoptotic cell morphology changes, we used additional approaches to prove that the outer ring of the EBs represents tuberin- and PRAS40-regulated apoptotic cell death. Hoechst propidium iodide (HOPI) staining to monitor apoptotic nuclear chromatin condensation demonstrated knockdown of PRAS40 or tuberin to trigger apoptosis represented by the induction of an outer EB ring of dead cells (Fig. 2A). Another common feature of apoptosis is cell shrinkage [for description and detection methods of apoptosis-specific hallmarks see (13)]. Cytofluorometric forward scatter (FSC) analyses demonstrated the induction of cell shrinkage in tuberin- or PRAS40-specific siRNA-treated EBs (Fig. 2B). Cytofluorometric DNA analyses were performed. These data demonstrated that the process of EB induction is accompanied by a G0/G1 cell cycle arrest of AFS cells. In addition, knockdown of PRAS40 or tuberin led to a significant increase in cells with the subG1 DNA content, representative for apoptosis-specific DNA fragmentation (Fig. 2C and D). Finally, we found the outer area cells to be positive for the apoptosis-specific cleavage of caspase 3 (Fig. 2E). Taken together, these studies of apoptotic events, such as cell morphological changes, nuclear chromatin condensation, cell shrinkage, DNA fragmentation and caspase 3 cleavage, allow the conclusion that both mTORC1 regulators, tuberin and PRAS40 are anti-apoptotic gatekeepers during EB formation of AFS cells.

The approach of HOPI staining also allows to discriminate between apoptotic and necrotic cells. Whereas PI uptake due to loss of membrane integrity is characteristic for both processes, Hoechst 33258 dye staining allows to detect apoptosis-specific chromatin condensation and nuclear fragmentation (13,14). To enable quantitative microscopical evaluation, we trypsinized the three-dimensional EBs to receive single cells. HOPI staining under these experimental conditions demonstrated that PRAS40 and tuberin knockdown triggers apoptosis, without induction of necrosis during EB formation of human AFS cells (Fig. 3A–C).

Next, we performed selective trypsinization procedures to separate the outer area cells (with typical apoptotic morphology) from the inner area cells of the studied EBs (Fig. 4A). FSC analyses of cell size demonstrated that within the inner area of the EBs, apoptosis-specific cell shrinkage was not elevated upon PRAS40- or tuberin (*TSC2*)-specific siRNA treatment. The mTOR pathway is the most important cell size regulating cascade in mammalian cells (10–12). These experiments also confirmed the well-known effects of the mTOR pathway on mammalian cell size regulation: knockdown of PRAS40 or tuberin triggered increased size of living cells. Within the cell pool obtained from selective isolation of the outer EB areas, pronounced cell shrinkage was detectable (Fig. 4B and C). Flow-cytometric analyses further revealed that within the outer EB areas, apoptosis-specific DNA fragmentation (analysed by the amount of subG1 cells) was significantly increased, whereas such an induction of this apoptotic feature was not observed in the inner areas (Fig. 4D and E). Again, it is important to mention that the siRNA treatment was started before EB formation was induced. Accordingly, siRNA-mediated downregulation of endogenous gene expression was achieved with the same efficiency in all cells, which later contributed to the three-dimensional EBs. For these experiments, the earlier established siRNA gene silencing protocol was used, which allows efficient gene knockdown in AFS cells for over 2 weeks (8,9). In summary, these data

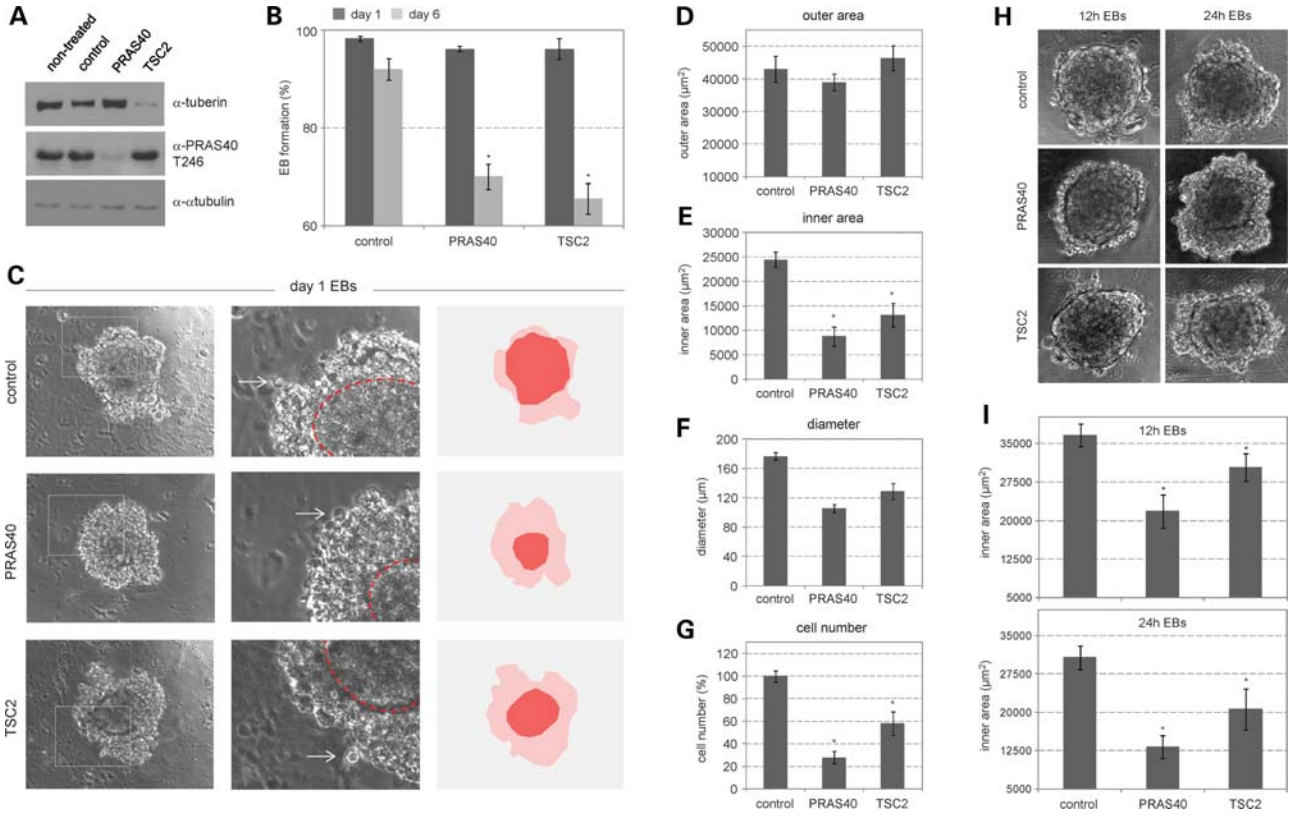

Figure 1. The role of tuberin and PRAS40 in EB development of AFS cells. (**A**) Monoclonal Q1 human AFS cells were transfected with non-targeting control siRNA, tuberin (*TSC2*)-specific siRNA or PRAS40-specific siRNA, and knockdown of endogenous tuberin and PRAS40 was confirmed by western blot analysis. α-Tubulin served as a control for equal loading. Lysates of non-transfected (non-treated) Q1 cells were analysed in parallel and were included to prove the used conditions of siRNA treatment to be physiologic and technically sound (compare control versus non-treated). (**B**) The number of EBs formed from the so-transfected cells was counted on day 1 (24 h post-induction of EB formation) and day 6 and the incidence of EB formation is given as a percentage of the number of cell aggregates initially seeded and induced to form EBs. (**C**) Left panel: representative bright-field pictures of day 1 EBs generated from differently transfected Q1 cells (magnification ×10). Middle panel: enlargement of the EB area marked in the left panel (arrows mark representative apoptotic cells). Right panel: schematic presentation of the inner area of the EB (dark red) and the outer area (light red). For detailed explanation see the text. (**D**) The whole area (outline of the outer area) of formed EBs was analysed at day 1. For each calculation, 10 EBs were photographed, the area was analysed via Cell D image software (Olympus) and the data are presented as average ± standard deviation. (**E**) The inner area (outline of the inner area) of formed EBs was analysed at day 1. For each calculation, 10 EBs were photographed, the area was analysed via Cell D image software (Olympus) and the data are presented as average ± standard deviation. (**F**) The mean diameter was deduced from measurements of the inner area of day 1 EBs. (**G**) The cell number of day 1 EBs (32 EBs for each calculation) was determined by a CASY cell counter and presented relative to the control. (**H**) Representative bright-field pictures of 12 h and 24 h EBs formed from Q1 cells transfected as indicated (magnification ×10). (**I**) The inner area of the EBs formed from transfected Q1 cells was analysed at the indicated time points. For all statistical analyses in this figure, Student's *t*-tests (unpaired, two-tailed) were performed and * indicates statistical significance with a *P*-value ≤ 0.05.

show the induction of the outer area during AFS cell EB formation to represent apoptosis mediated by endogenous knockdown of the mTOR inhibitors PRAS40 or tuberin.

Downregulation of endogenous tuberin or PRAS40 is without effects on germ layer-specific marker expression

Starting from one single AFS cell, the formation of EBs, composed of cells of all three germlayers, is induced. This AFS cell-derived EB formation is accompanied by a decrease in the expression of the stem-cell markers nodal and Oct-4 and by induction of the differentiation markers Pax 6 (ectodermal), Flk1 (endothelial), E-cadherin (epithelial), GATA4 (endodermal), T (brachyury; mesodermal) and HBE1 (mesodermal). AFS cell-derived EBs are also positive for laminin and nestin. In addition, as for ES cell-derived EBs, AFS cell-derived EBs also form the characteristic distinct peripheral layer on the outer surface, including cells expressing α-fetoprotein (αFP) (8).

Accordingly, it was interesting to investigate whether the above-described apoptotic effects of PRAS40 or tuberin knockdown were accompanied by effects on the cell differentiation spectrum within the EBs. We immunocytochemically analysed the expression of the mesodermal marker Wilms tumor 1 (WT1) (5,15), of the endodermal marker αFP (8,16) and of the ectodermal marker nestin (4,16). Specificity of the used antibodies was confirmed by analyzing αFP-negative IMR-90 fibroblasts (17), αFP-positive Hela cells (18) (Supplementary Material, Fig. S1A), nestin-negative Jurkat cells and nestin-positive SK-N-SH cells (19) (Supplementary Material, Fig. S1B), WT1-negative MCF-7 cells (20) and WT1-positive embryonic kidney cells (5,21) (Supplementary Material, Fig. S1C). We found that although the size of the inner area EBs decreased, neither PRAS40 knockdown nor tuberin

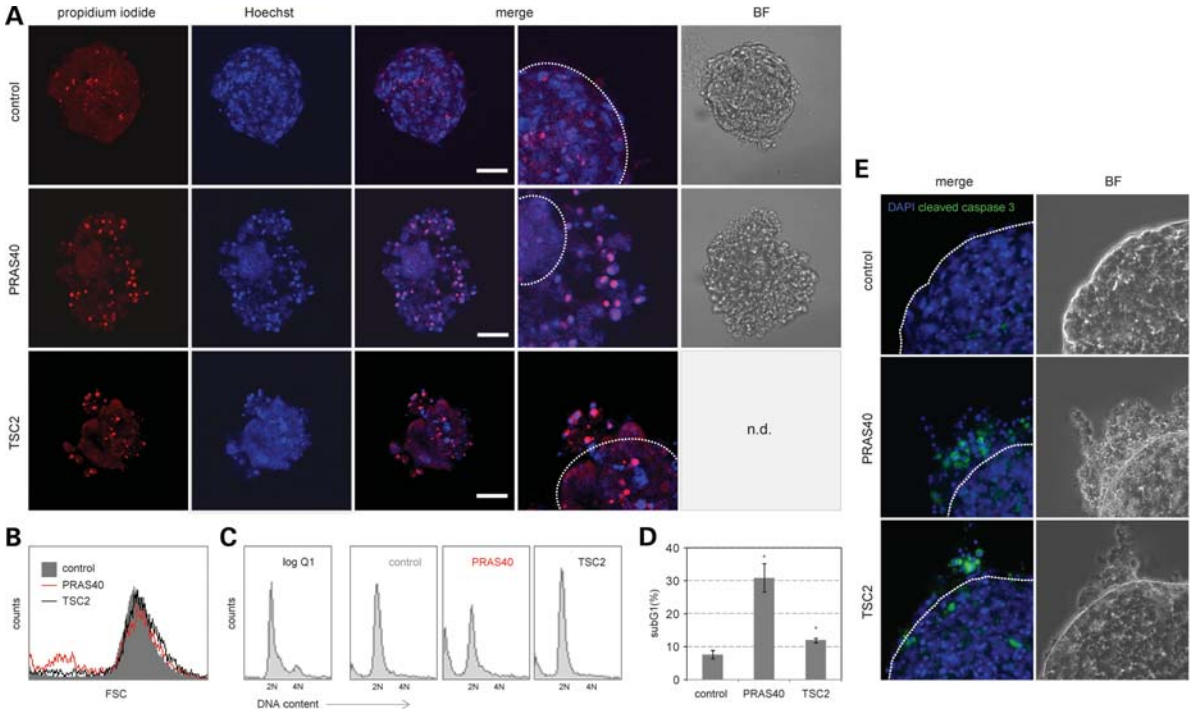

Figure 2. Knockdown of endogenous tuberin or PRAS40 triggers apoptosis during EB development of AFS cells. (**A**) Day 1 EBs, derived from siRNA-treated Q1 cells as described in Figure 1, were stained with HOPI for 1 h at 37°C and then analysed on a confocal microscope (magnification ×25). Scale bars represent 50 μm. In addition, enlarged pictures (the white dotted line marks the boundary between inner and outer area) and bright-field pictures are presented. (**B**) Day 1 EBs were trypsinized and relative cell size was studied via cytofluorometric FSC analyses. A representative overlay of FSC histograms is presented. (**C**) In the same samples, apoptotic cells were cytofluorometrically detected by their subG1 DNA content (DNA content <2N). Representative DNA profiles are presented. The log Q1 picture represents non-transfected Q1 cells logarithmically growing in petri dishes without induction of EB formation. (**D**) Quantitative investigation of the amount of subG1 cells in EBs analysed in (C). Student's *t*-test was performed and * indicates statistical significance (*P*-value ≤ 0.05; $n = 3\times$ 96-well plate). (**E**) Immoncytochemical detection of cleaved caspase 3 in the so-formed EBs (the white dotted line marks the boundary between inner and outer area).

knockdown affected the expression pattern of the studied mesodermal, endodermal or ectodermal markers within the EBs (Fig. 5). These findings provide evidence that these two mTOR inhibitors are anti-apoptotic gatekeepers during early AFS cell differentiation, but are not involved in lineage-specific regulations of differentiation.

So far, in the study presented here, we have proved that the outer cells (appearing upon siRNA-knockdown of tuberin or PRAS40) are apoptotic rather than, for example, differentiating (analyses of cell shrinkage, DNA fragmentation, chromatin condensation, caspase 3 cleavage). In addition, these marker stainings confirm that the outer cells are not differentiating since they are, for example, αFP negative (see the enlarged pictures of αFP staining in Fig. 5).

Downregulation of endogenous tuberin or PRAS40 does not induce apoptosis in two-dimensionally growing AFS cells

To investigate whether the described apoptotic effects of siRNA-mediated knockdown of tuberin or PRAS40 specifically occur in the course of cell differentiation processes during EB formation, we performed experiments in two-dimensionally (2D) growing AFS cells. Downregulation of endogenous tuberin or PRAS40 in AFS cells growing in 2D and high serum (Fig. 6A and B) had neither effects on the cell morphology (Fig. 6A), on chromatin condensation analysed by HOPI staining (Fig. 6C), on cell shrinkage flow-cytometrically investigated by FSC analyses (Fig. 6D), on DNA degradation studied by subG1 analyses (Fig. 6E) nor on caspase cleavage analysed by western blot (Fig. 6F). These results demonstrate that the apoptotic effects of tuberin- or PRAS40-knockdown specifically occur in the course of EB formation.

In the western blot analyses of caspase 3 cleavage, we co-analysed protein extracts obtained upon EB formation as apoptotic controls (Fig. 6F). Once again, these experiments confirmed the EB-specific apoptotic effects of knockdown of both tuberin and PRAS40. These western blot analyses of caspase 3 cleavage also provided evidence that the effects of PRAS40 are more severe than the effects of tuberin knockdown (Fig. 6F). Although all the data obtained in this study demonstrate that tuberin is also an anti-apoptotic gatekeeper during stem-cell differentiation, the effects of PRAS40 modulation appeared to be more pronounced in all performed experiments (see especially Figs 1, 2 and 4). Although the efficiency of siRNA-mediated downregulation of PRAS40 and tuberin in AFS cells seemed always to be very comparable (Figs 1A and 6B), it is still hard to say whether these differences are a consequence of different starting levels of PRAS40 and tuberin protein amounts or are due to different biochemical functions of these two regulators.

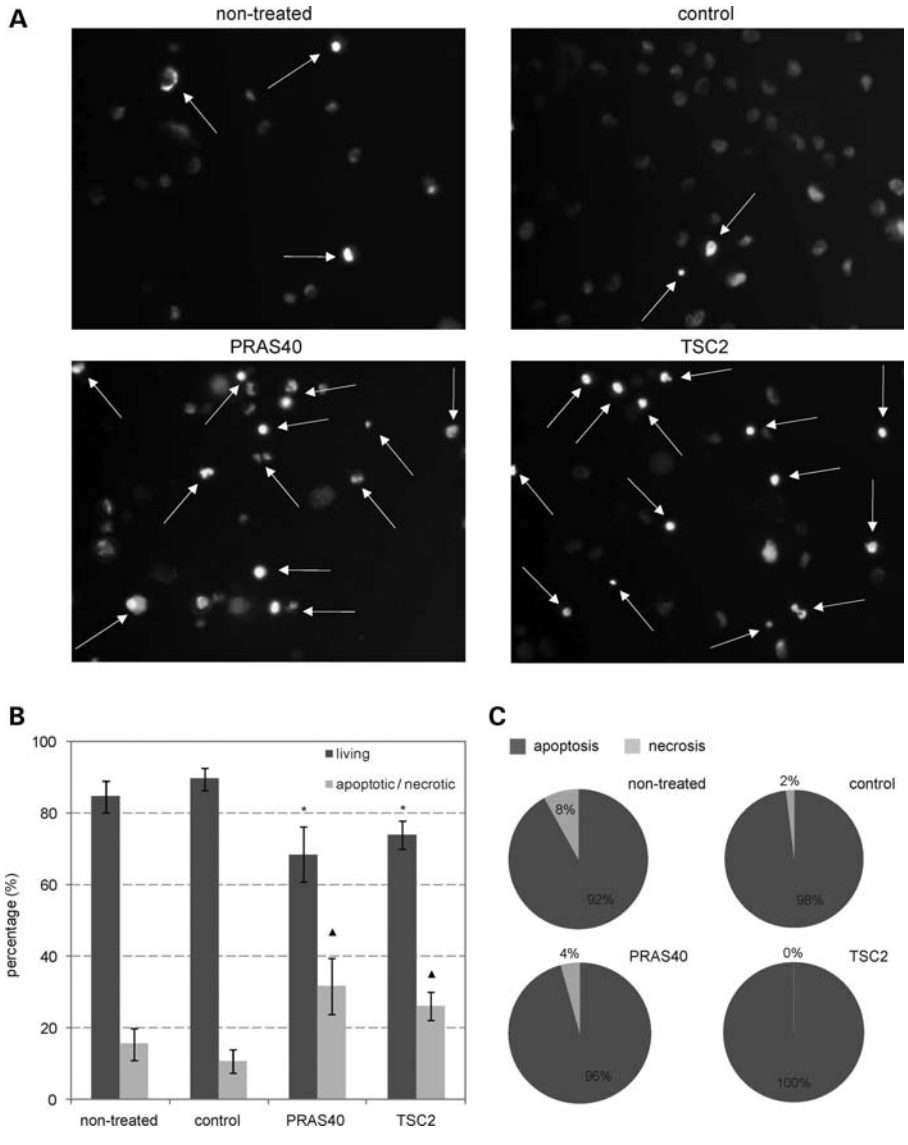

Figure 3. Downregulation of endogenous tuberin or PRAS40 triggers apoptosis, but not necrosis, during EB formation of AFS cells. (**A**) Day 1 EBs formed from Q1 cells, siRNA-transfected as indicated, were trypsinized to receive single cells and stained with HOPI to monitor nuclear chromation condensation and cell death (arrows) (magnification $\times 20$). In parallel, Q1 cells left untreated and formed into EBs were co-analysed to prove the used conditions of siRNA treatment to be physiologic and without any significant cytotoxic effects (compare control versus non-treated). (**B**) Living and apoptotic/necrotic cells were counted upon HOPI staining and data are presented as average $\pm$ standard deviation. Statistical analyses were performed via Student's *t*-tests and * or $\triangle$ indicates a *P*-value ≤ 0.05 compared with living control cells (*) or dead control cells ($\triangle$) ($n \geq 500$ cells per condition). (**C**) HOPI-positive (apoptotic/necrotic) cells were analysed for chromatin morphology and further graded into apoptotic and necrotic cells (for details see Materials and Methods).

The apoptotic effects of tuberin and PRAS40 are mTOR dependent

Akt-mediated phosphorylation of tuberin downregulates its GTPase-activating potential toward Rheb, which is a potent regulator of mTORC1 (10–12). However, a wide variety of mTORC1-independent functions of tuberin, such as its potential to regulate the cyclin-dependent kinase inhibitor p27 (22), have also been described (23). PRAS40 binds to raptor and inhibits the function of mTORC1 (12,24–26). Still, it has also been suggested that PRAS40 is an mTORC1 substrate (26–28). Accordingly, it was important to clarify whether the described potentials of tuberin and PRAS40 are mediated via mTOR.

The most commonly used approach to modify mTOR activity is via its inhibitor rapamycin (10,11). We therefore wanted to investigate whether rapamycin could revert the apoptotic consequences of the endogenous knockdown of the studied mTORC1 inhibitors. However, rapamycin treatment did not affect the potential of PRAS40 or tuberin to regulate apoptosis during EB formation of AFS cells, as demonstrated by the investigation of the inner area and cell number of PRAS40- or tuberin-depleted EBs in the presence or absence of rapamycin (Fig. 7). It is known that there exist rapamycin sensitive and insensitive functions of mTORC1, with regard to its major substrates p70S6K and 4EBP1 (10–12,29). mTORC1-mediated phosphorylation and activation of p70S6K is immediately and

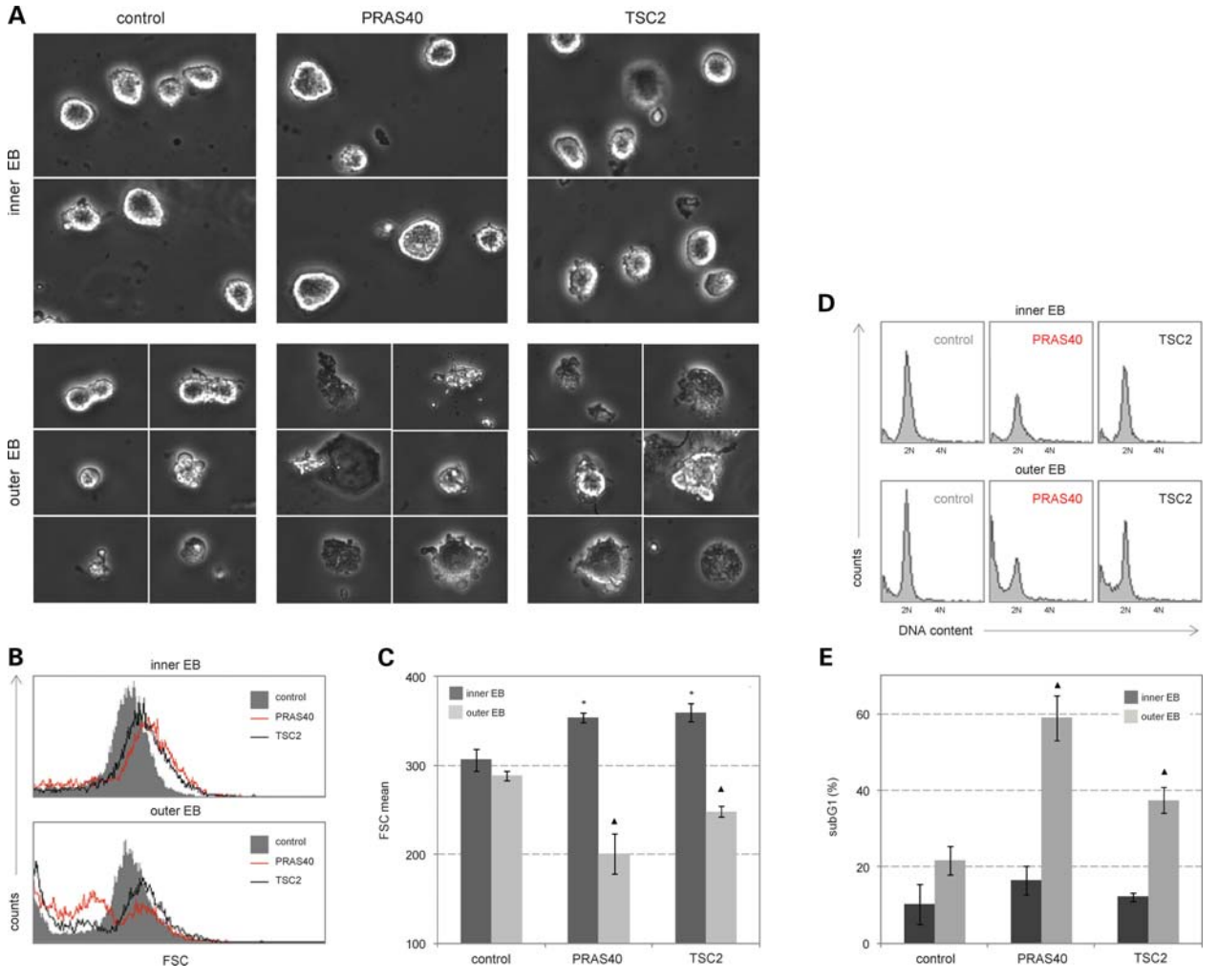

Figure 4. The outer area of AFS cell EBs represents apoptosis induced by tuberin or PRAS40 knockdown. (**A**) Day 1 EBs of control, PRAS40 or tuberin (*TSC2*)-siRNA-transfected Q1 cells were first shortly trypsinized to harvest the outer cells and in a second step for the inner EB cells (for the exact cell separation procedure see Materials and Methods). Bright-field pictures of cells from the inner and outer area of the EBs are presented. (**B**) Cell size (cell shrinkage represents dead cells) was cytofluorometrically investigated by FSC analyses. Representative overlays of FSC histograms are shown. (**C**) Comparison of the relative cell size (FSC mean) of inner and outer cells in differently siRNA-transfected EBs (P-value ≤ 0.05; Student's t-test $n = 3\times$ 96-well plate). (**D**) Cytofluorometrical analysis of apoptotic subG1 cells with fragmented DNA within the inner and the outer area of EBs from control, PRAS40 or tuberin (*TSC2*)-siRNA-transfected Q1 cells. Representative DNA profiles are shown. (**E**) Analysis of the percentage of subG1 cells within the inner and outer areas of differently transfected EBs (P-value ≤ 0.05; Student's t-test $n = 3\times$ 96-well plate).

potently inhibited via addition of rapamycin (30,31) (Fig. 7A). However, after an initial block, within some hours, 4EBP1 activity becomes resistant to rapamycin (29). Co-knockdown experiments using mTOR-specific siRNA clearly demonstrated the effects of PRAS40 and tuberin on the apoptosis regulation in AFS cell EBs to be mTOR dependent, as evaluated by measurements of the inner area and cell number of PRAS40- or tuberin-depleted EBs with or without concomitant knockdown of mTOR (Fig. 8). Taken together, these results show that both tuberin and PRAS40 are major anti-apoptotic regulators during early AFS cell differentiation due to their potential to control the rapamycin-insensitive functions of mTOR.

DISCUSSION

EB formation is a commonly used *in vitro* model to investigate stem-cell differentiation processes mimicking early embryogenesis (6,7). It has already earlier been shown that mTOR plays a role for EB formation processes (8,32), but the underlying mechanism remained elusive. Here, we demonstrate that the two mTOR regulators, tuberin and PRAS40, are anti-apoptotic gatekeepers during EB formation due to their potential to regulate rapamycin-insensitive mTOR functions.

Tuberin is the gene product of *TSC2*, which when mutated causes TSC, a multisystem disorder affecting ~1 in 6000 live births. It is characterized by the development of tumor-like growths in the kidneys, heart, skin and brain, dermatological manifestations, epilepsy, mental retardation and autism. With regard to the molecular development of this human genetic disease many questions connected with the tissue specificity of tumor development are still under investigation (23,33). We provide the first description of a connection between stem-cell activities and tuberin, with clear implications for future

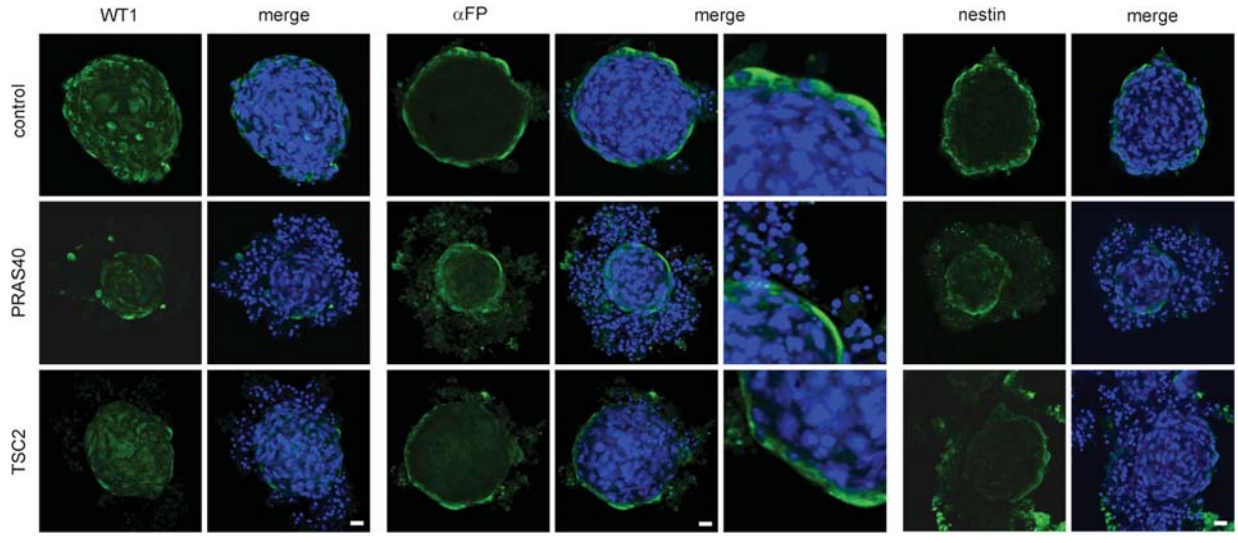

Figure 5. Knockdown of endogenous tuberin or PRAS40 is not affecting germ layer-specific marker expression. Monoclonal Q1 AFS cells were transfected with non-targeting control, PRAS40- or tuberin (*TSC2*)-specific siRNA. Day 1 EBs were immunocytochemically analysed for marker expression (WT1-mesoderm; αFP-endoderm; nestin-ectoderm). Nuclei were counterstained with DAPI in blue (magnification ×25). Scale bars represent 20 μm. In case of αFP staining, enlarged pictures are shown additionally.

studies on the molecular processes of TSC development. Also for PRAS40, a role in stem-cell maintenance has not been reported before. Deregulation of PRAS40 activity has been implicated to play a role in the development of breast cancer, lung cancer, meningiomas and melanomas (34). Mutations and deregulations of mTOR pathway components have been demonstrated to be involved in the human genetic diseases, TSC, Peutz–Jeghers syndrome, Cowden syndrome, Bannayan–Riley–Ruvalcaba syndrome, Lhermitte–Duclos disease, Proteus syndrome, von Hippel–Lindau disease, neurofibromatosis, polycystic kidney disease, in several sporadic tumors, as well as in Alzheimer's disease, cardiac hypertrophy, obesity and type 2 diabetes (33). Our data warrant future studies to investigate the question to which extent the described effects of tuberin and PRAS40 on stem-cell activities might be involved in the molecular development of these diseases.

The reported findings suggest that both tuberin and PRAS40 are indispensable during early mammalian stem-cell differentiation and development. Whereas PRAS40 knockout in animals has not been reported so far, *TSC2*−/− mice are known to die at E9.5–E12.5 due to a variety of malformations and dysfunctions (35,36). Not surprisingly, mTOR knockout is also lethal during early murine embryonic development (37,38). Interestingly, however, upon injection of the mTOR inhibitor rapamycin at E5.5–E8.5, most mouse embryos develop normally. Upon these observations, the authors concluded that the rapamycin-insensitive function of mTOR is the relevant trigger for proper embryonal development (37–41). Our results are in perfect agreement with this assumption. Treatment with mTOR-specific siRNA but not with rapamycin could revert the apoptotic effects of endogenous knockdown of tuberin or PRAS40 during EB formation of AFS cells. Accordingly, our findings also highlighted the relevance of the rapamycin-insensitive mTOR functions for early development.

Although without effects on the mesodermal, endodermal and ectodermal cell differentiation spectrum in the EBs, we detected knockdown of tuberin or PRAS40 to trigger a strong induction of apoptosis, as proved by the detection of cell morphological changes, cell shrinkage, nuclear chromatin condensation and DNA fragmentation. Downregulation of PRAS40 activity has already earlier been shown to associate with an increased sensitivity of tumor cells to pro-apoptotic stimuli (42). Here, we demonstrate that this mechanism is obviously also active in human stem cells. Although never investigated in stem cells, in the past, tuberin has been shown to mediate both pro- and anti-apoptotic effects, likely depending on the cell type and on the exogenous triggers (13,43–46). In this study, we found tuberin to play an essential anti-apoptotic role during early human stem-cell differentiation. Inoki *et al.* (43) reported that AMP-activated protein kinase phosphorylates tuberin on residues T1227 and S1345, what protects cells from energy deprivation-triggered apoptosis. Tuberin is further known to induce apoptosis via its ability to negatively regulate p70S6K, what activates BCL2-associated agonist of cell death to promote cell death (13,44). Different groups have already earlier shown that tuberin can mediate anti-apoptotic effects in an mTOR-dependent manner (43,45,46). Rapamycin sensitive and insensitive functions of mTORC1 have been described (10–12,29,46,47). One study has already demonstrated an anti-apoptotic function of tuberin, which is rapamycin insensitive, but depends on mTOR (46). This study is the first to demonstrate tuberin's role in the regulation of apoptosis in stem cells and shows this anti-apoptotic function to also depend on the rapamycin-insensitive mTOR function.

In conclusion, this report shows for the first time that tuberin and PRAS40 play a role in stem-cell biology. It is the first description that early human AFS cell differentiation is regulated/controlled via apoptosis. In fact, almost nothing is known about the role of apoptosis during EB formation of

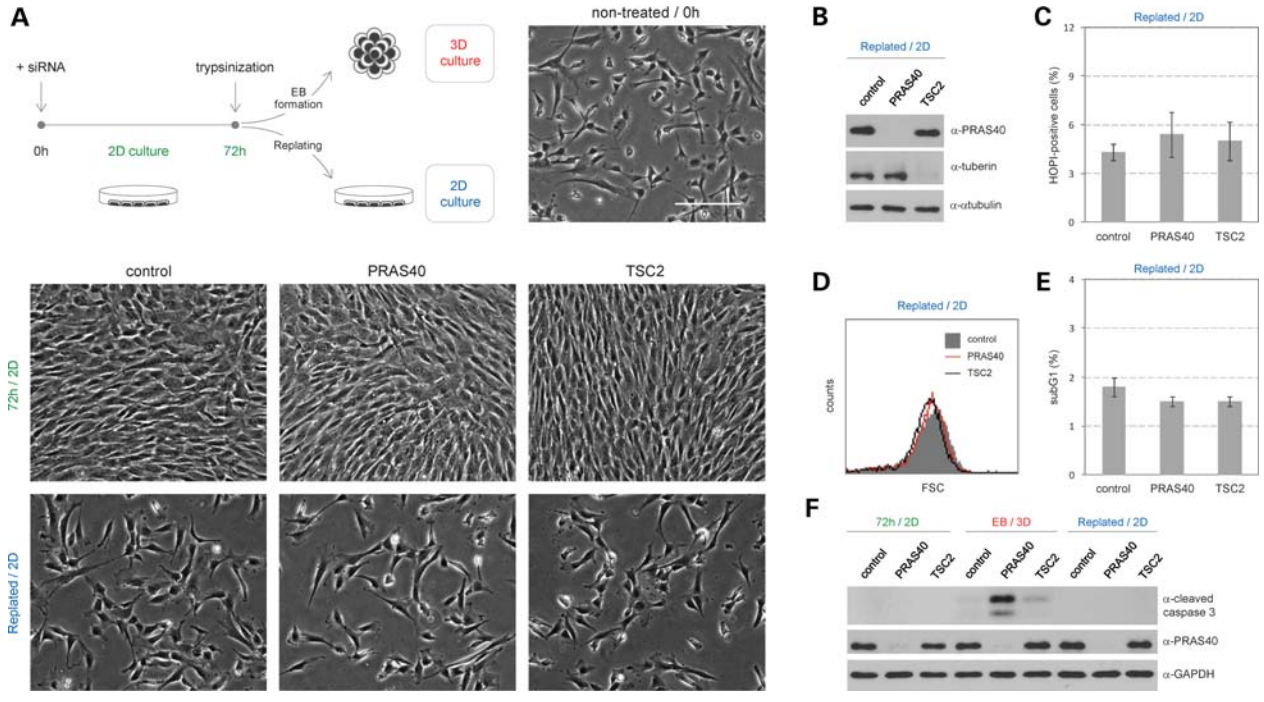

Figure 6. Knockdown of endogenous tuberin or PRAS40 does not trigger apoptosis in two-dimensionally growing AFS cells. (**A**) Monoclonal Q1 human AFS cells were transfected with non-targeting control siRNA, tuberin (*TSC2*)-specific siRNA or PRAS40-specific siRNA. Instead of using these cells for EB formation, in this study, the cells were replated under 2D cell culture conditions. A schematic presentation of the used experimental approach, a bright-field picture of non-treated AFS cells and bright-field pictures of the siRNA-treated AFS cells before and after replating are shown. (**B**) Knockdown of endogenous tuberin and PRAS40 was confirmed by western blot analysis. α-Tubulin served as a control for equal loading. These cells, replated and grown in 2D, were investigated by (**C**) HOPI staining (chromatin condensation), by (**D**) cytofluorometric FSC analyses (cell shrinkage), by (**E**) cytofluorometric subG1 analyses (DNA degradation) and by (**F**) western blot detection of caspase 3 cleavage (parallel analyses of EB-derived protein extracts served as apoptotic-positive controls). Glyceraldehyde 3-phosphate dehydrogenase (GAPDH) served as a control for equal loading.

stem cells in general, and a connection to tuberin or PRAS40 has never been drawn before. The latter is of special interest, since, as described above, the loss of endogenous tuberin or PRAS40 is involved in the pathogenesis of human genetic disease and cancer. In addition, this report contains the first description of a PRAS40-mediated anti-apoptotic potential via rapamycin-insensitive mTOR. And finally, our study contains the technical confirmation that EB formation of AFS cells combined with siRNA-mediated gene knockdown is an invaluable tool to study the role of endogenous gene functions for the three-dimensional and tissue level context of stem-cell differentiation processes mimicking early mammalian embryogenesis.

MATERIALS AND METHODS

Cell culture

The human AFS cell line Q1 has been established by Anthony Atala via magnetic cell sorting using the CD117 MicroBead Kit (4). AFS cells were grown in the α-MEM minimal essential medium (Invitrogen, Carlsbad, CA, USA, 41061), supplemented with 15% fetal bovine serum (HyClone, Waltham, MA, USA, 30070.03), 18% Chang B, 2% Chang C (Irvine Scientific, CA, USA, C100, C106), 2 mM L-glutamine, 50 mg/l streptomycin sulfate and 30 mg/l penicillin. The human non-transformed, non-immortalized, primary fetal lung fibroblasts IMR-90 were grown in the Dulbecco's modified Eagle medium-high glucose (DMEM-HG) medium. The cell lines MCF-7 (mammary gland adenocarcinoma) and Hela (epithelial cervix carcinoma) were also grown in the DMEM-HG medium supplemented with 10% fetal calf serum (FCS) and antibiotics (30 mg/l penicillin, 50 mg/l streptomycin sulfate) and 2 mM L-glutamine. Jurkat cells (human T cell leukemia) are suspension cells and were grown in the DMEM-HG medium supplemented with 10% FCS and 2.5 mM L-glutamine. SK-N-SH cells (human neuroblastoma) were cultured in the Roswell Park Memorial Institute (RPMI) medium supplemented with 20% FCS and 2 mM L-glutamine. Cells used for immunofluorescence staining were seeded and cultured on either glass or permanox slides. Mouse embryonic kidneys (E11.5) were dissected, grown and stained as described (5). Cells were cultivated at 37°C and 5% CO_2 and were routinely screened for mycoplasma via DAPI staining and polymerase chain reaction (PCR) (EZ-PCR mycoplasma test kit, Biological Industries, 20-700-20). The mTOR inhibitor rapamycin (Calbiochem, La Jolla, CA, USA, 553211) was added to cells at a final concentration of 100 nM.

EB formation

EBs were generated using a suspension method with 0.3% (w/v) methylcellulose in 96-well plates with a U shape and non-adhesive cell culture plastic (PAA, Pasching, Austria,

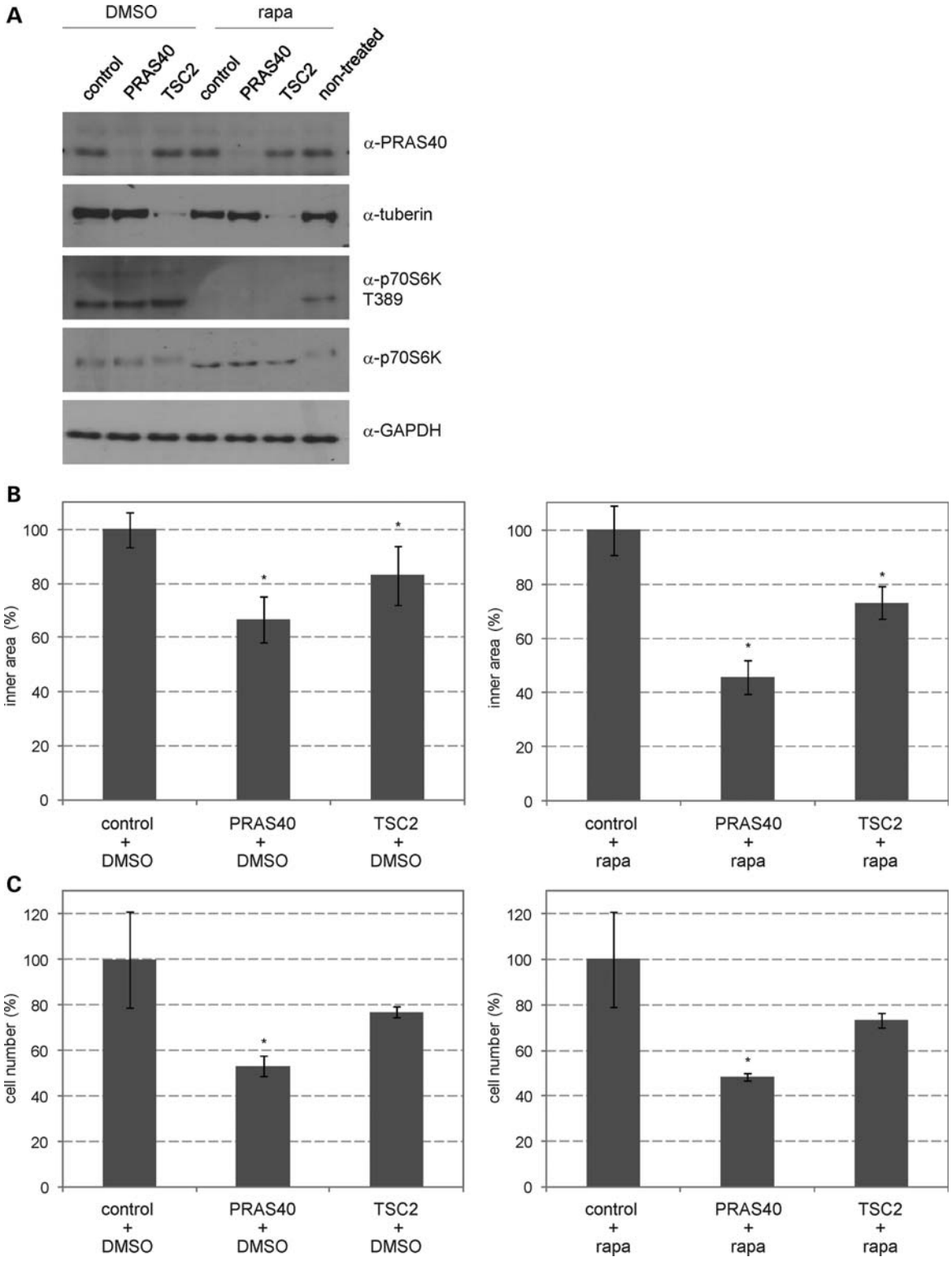

Figure 7. Knockdown of tuberin or PRAS40 causes apoptosis in AFS cell EBs treated with the mTOR inhibitor rapamycin. (**A**) Q1 AFS cells were transfected with non-targeting control siRNA, PRAS40 siRNA or tuberin (*TSC2*) siRNA. Forty-eight hours after transfection, cells were treated with 100 nM rapamycin or vehicle (DMSO). Efficient knockdown of PRAS40 or tuberin protein was confirmed by western blot analysis 72 h after transfection. Additionally, the negative effects of rapamycin on mTORC1 activity were confirmed by analyzing the phosphorylation status of p70S6K T389. GAPDH served as a control for equal loading. Lysates of non-transfected (non-treated) Q1 cells were analysed in parallel and were included to prove the used conditions of siRNA treatment to be physiologic and technically sound (compare control versus non-treated). (**B**) The inner area (outline of the inner area) of formed day 1 EBs was analysed. For each calculation 10 EBs were photographed, the area was analysed via Cell D image software (Olympus) and the data are presented as average ± standard deviation (control set to 100%). (**C**) The cell number of these EBs (32 EBs for each calculation) was determined by a CASY cell counter. For all statistical analyses in this figure Student's *t*-tests (unpaired, two-tailed) were performed and * indicates statistical significance with a *P*-value ≤ 0.05.

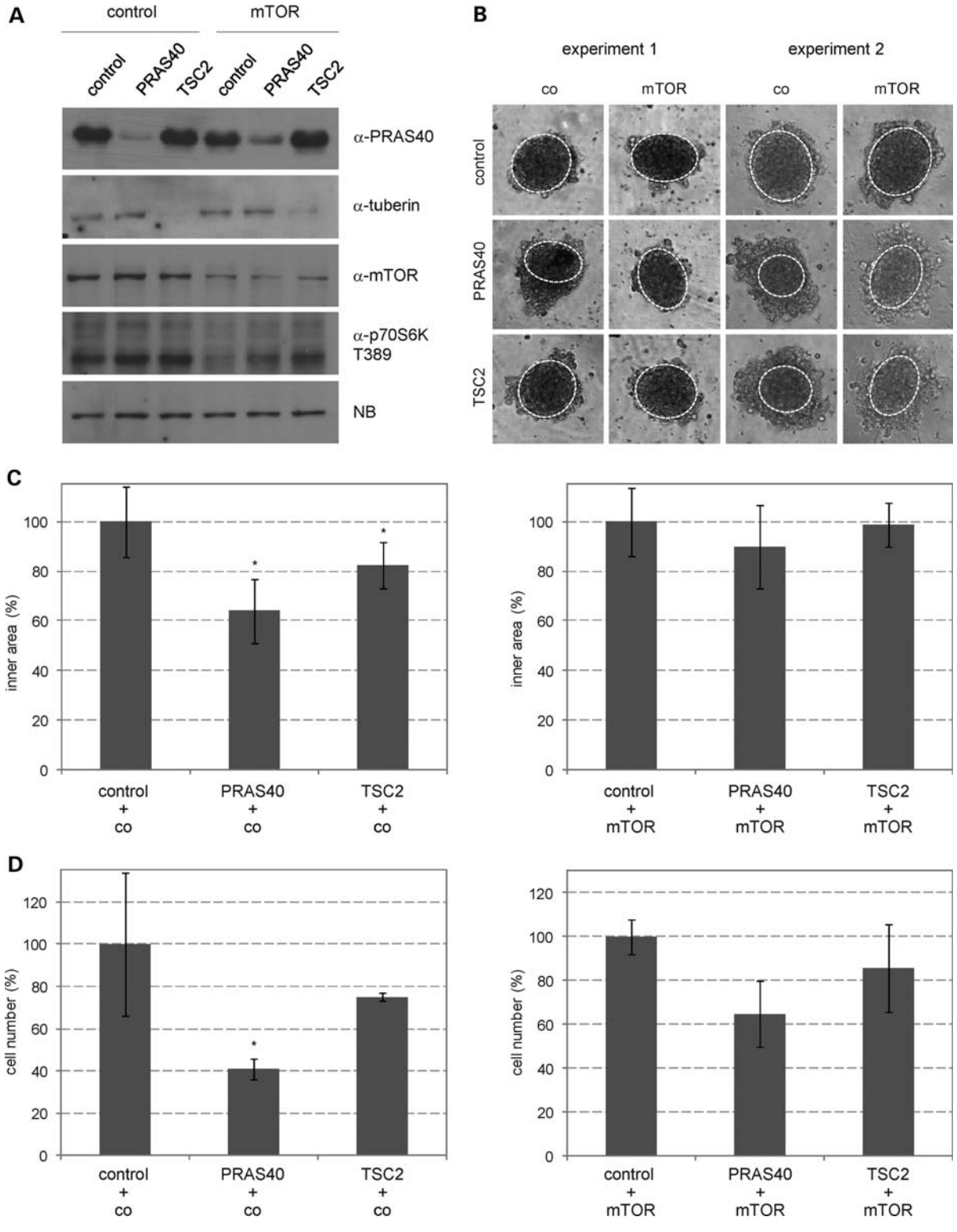

Figure 8. The apoptotic effects of tuberin or PRAS40 knockdown depend on mTOR. (**A**) Q1 AFS cells were transfected with non-targeting control siRNA, PRAS40 siRNA or tuberin (*TSC2*) siRNA and were co-transfected with either control or mTOR-specific siRNA. Knockdown of endogenous PRAS40, tuberin or mTOR was confirmed by western blot analysis 72 h after transfection. Additionally, the mTORC1-dependent phosphorylation status of p70S6K T389 was analysed. A non-specific band served as a control for equal loading. (**B**) Bright-field pictures of the formed EBs are shown. (**C**) The inner area (outline of the inner area) of formed day 1 EBs was analysed. For each calculation, 10 EBs were photographed, the area was analysed via Cell D image software (Olympus) and the data are presented as average ± standard deviation (control set to 100%). (**D**) The cell number of these EBs (32 EBs for each calculation) was determined by a CASY cell counter. For all statistical analyses in this figure, Student's *t*-tests (unpaired, two-tailed) were performed and * indicates statistical significance with a P-value ≤ 0.05.

34296X) as described (8). A single EB is composed of 1000–1500 cells in 100 μl medium. For analysis of cell number, cell size, DNA content and protein expression of whole EBs, EBs were directly harvested, washed three times in ice-cold 1× phosphate buffered saline (PBS) and then trypsinized for 15–20 min to receive a single cell suspension. Separating the inner and outer cells of EBs was achieved by harvesting EBs, washing them carefully with ice-cold 1× PBS, followed by 2–3 min incubation with trypsin-EDTA (TE). Reaction was stopped by adding serum-containing medium to EBs. EBs and single cells (outer cells) were separated by slow centrifugation (300 rpm, 5 min, 4°C). Supernatant was collected, transferred into new tubes and centrifuged for 10 min at 1000 rpm and at 4°C. The cell pellet was then used for further analysis. Remaining EBs were washed with 1× PBS and then trypsinized for 15–20 min to receive single cells (inner cells). So obtained cell pellets were further processed for analysis.

siRNA treatment

RNA silencing was achieved using siRNA specific for human PRAS40, tuberin and mTOR (ON-TARGETplus SMART pool reagents, Dharmacon, Lafayette, CO, USA) at a final concentration of 50 nM (9). siRNA was delivered to cells using Lipofectamine RNAiMAX reagent (Invitrogen). A pool of four non-targeting siRNAs was used as control for non-sequence-specific effects for each transfection. In experiments, where single knockdowns were compared with the simultaneous knockdown of two genes, the amount of gene-specific siRNA was reduced to 25 nM while keeping the overall amount of siRNA for each reaction (50 nM) constant by adding non-targeting siRNA. EB formation of siRNA-treated cells was performed 72 h after transfection.

Flow cytometry and CASY cell counter

Single cells from 2D cultures (cells grown on plates) and 3D cultures (whole EB, inner EB and outer EB) were fixed by rapid submersion in ice-cold 85% ethanol. After fixation overnight at −20°C, DNA was stained with 0.25 mg/ml propidium iodide (PI), 0.05 mg/ml RNAse A, 0.1% Triton X-100 in citrate buffer, pH 7.8 and relative cell size (FSC), and DNA content and subG1 fraction were analyzed on a Beckton Dickinson FACSCalibur (Beckton Dickinson, San Jose, CA, USA) (48). For flow-cytometric analysis, a 96-well plate with EBs was used in triplicate. For cell number determination, EBs were trypsinized to obtain single cells and the number of vital cells was analysed on a CASY Cell Counter (Innovatis, Roche, Basel, Switzerland). For each measurement, 32 EBs were trypsinized to calculate the cell number of a single EB. Measurements were performed in triplicate.

Microscopy and area measurement

For phase contrast images, EBs were photographed with an Olympus IX51 equipped with a XC50 camera (Olympus, Tokio, Japan). For the measurements of the 'inner area' and 'whole area' of EBs, pictures were randomly taken from three 96-well plates and the area was determined using the microscopic imaging software Cell^D (Olympus). The inner area of the EB is defined as the round-shaped inner structure. The cells situated out of the inner EB are integrated in the measurement of the 'whole EB' (for a scheme see Fig. 1C). The mean diameter of the EB was deduced from measurements of the inner area of day 1 EBs (24 h after induction of EB formation). All immunostained samples were analysed on either an Olympus IX51 microscope with a XC50 camera (Olympus) or a Zeiss LSM Exciter confocal microscope (Carl Zeiss, Oberkochen, Germany). The microscopes were not changed within one experiment.

Immunocytochemistry

Cells on slides were fixed in 4% paraformaldehyde for 10 min at room temperature. Fixed cells were washed with PBS and then permeabilized in 0.1% Triton X-100 in PBS (PBS/T) for 10 min, followed by blocking with 0.5% bovine serum albumin in PBS/T for 30 min at room temperature. Cells were subsequently incubated with primary antibody overnight at 4°C. Antibodies specific for the following proteins were used: anti-αFP antibody (R&D Systems, Minneapolis, MN, USA, MAB4305), anti-laminin antibody (Sigma, St Gallen, Switzerland, L9393), anti-nestin antibody (Neuromics, Edina, MN, USA, MO15012) and anti-WT1 antibody (Dako, Glostrup, Denmark, M3561). Thereafter, cells were washed with PBS and incubated with labeled secondary antibody (1:100 in PBS) for 30 min at room temperature: goat tetramethyl rhodamine iso-thiocyanate α-rabbit (Sigma) or goat fluorescein iso-thiocyanate α-mouse (Sigma). Cells were washed again and DAPI (4,6-diamino-2-phenylindole; 1 μg/ml) was added for nuclei staining.

EBs were incubated with 4% paraformaldehyde for 30 min at room temperature and then carefully washed with PBS, followed by washing 15 min in 0.1% Triton X-100 in TBS (TBS/T) and subsequently 15 min in PBS/T. EBs were blocked for 1 h in 1% BSA in PBS/T. EBs were washed and incubated with primary antibody overnight at 4°C. Antibodies specific for the following proteins were used: cleaved caspase 3, Asp175 (clone 5A1E) (Cell Signaling, Danvers, MA, USA, 9664), αFP (R&D Systems), nestin (Neuromics) and WT1 (Dako). After primary antibody incubation, EBs were washed and afterwards stained with labeled secondary antibodies: Alexa Fluor 488 goat α-mouse (Molecular Probes, Invitrogen, A11029) or Alexa Fluor 488 goat α-rabbit (Molecular Probes, Invitrogen, A11034) and DAPI overnight at 4°C. The next day, stained EBs were washed three times with 1× PBS and then transferred onto glass slides. Images were obtained with a Zeiss LSM Exciter confocal microscope (Carl Zeiss).

HOPI staining

The cell culture medium with a final concentration of 5 μg/ml Hoechst 3358 dye (HO) and 2 μg/ml PI was prepared. For analysis of cells from 2D cultures (cells grown on plates) and 3D cultures (whole EB), cells/EBs were washed with PBS and treated with TE (for dissociation of whole EBs, EBs were processed as described above). The trypsinized, single cells were harvested in an Eppendorf tube and incubated

with the HOPI stain for 1 h at 37°C. After incubation, the cells needed to be carefully resuspended to receive a single cell solution, were put on a glass slide and pictures were taken with the Olympus microscope (up to 10 pictures per sample). EBs without prior dissociation were directly incubated with the HOPI dye in a 96-well plate and were analyzed on a confocal microscope after 1 h incubation. The analysis of stained, single cells was done by counting viable, apoptotic and necrotic cells. The Hoechst 33258 dye stains the nuclei of all cells. Nuclear changes, such as chromatin condensation and nuclear fragmentation, are associated with apoptosis. PI uptake indicates the loss of membrane integrity being characteristic for necrosis and apoptosis. Necrosis is characterized by nuclear PI uptake into cells without chromatin condensation or nuclear fragmentation (14).

Protein extraction

Total protein of cells from 2D cultures (cells grown on plates) and 3D cultures (whole EB) was extracted by physical disruption of cell membranes by repeated freeze and thaw cycles. In brief, cells/EBs were harvested by trypsinization to receive single cells (for dissociation of whole EBs, EBs were processed as described above). Cell pellets were washed with PBS and lysed in buffer A containing 20 mM Hepes, pH 7.9, 0.4 M NaCl, 25% glycerol, 1 mM EDTA, 0.5 mM dithiothreitol, 1 mM phenylmethylsulfonyl fluoride, 0.5 mM NaF, 0.5 mM Na_3VO_4 supplemented with 2 μg/ml aprotinin, 2 μg/ml leupeptin, 0.3 μg/ml benzamidinchlorid, 10 μg/ml trypsininhibitor by repeated freeze and thaw cycles. After incubation on ice and centrifugation at 15000 rpm for 20 min at 4°C, supernatants were collected and protein lysates stored at −80°C. Protein concentrations were determined using the Bio-Rad protein assay (22).

Immunoblotting

Proteins (7–15 μg/lane) were run on a sodium dodecyl sulfate-polyacrylamide gel and transferred onto a nitrocellulose membrane. Blots were stained with Ponceau-S to visualize the amount of loaded protein. For immunodetection, antibodies specific for the following proteins were used: tuberin C-20 (Santa Cruz Biotechnology, Santa Cruz, CA, USA, sc-892), phospho-PRAS40 T246 (Cell Signaling, 2997), PRAS40 (clone D23C7) (Cell Signaling, 2691), mTOR (Cell Signaling, 2972), phospho-p70S6K T389 (clone 108D2) (Cell Signaling, 9234), p70S6K (Cell Signaling, 9202), cleaved caspase 3, Asp175 (clone 5A1E) (Cell Signaling, 9664), α-tubulin (clone DM1A) (Calbiochem, CP06) and glyceraldehyde 3-phosphate dehydrogenase (GAPDH) (Trevigen, Gaithersburg, MD, USA, 2275-PC-100). Rabbit polyclonal and monoclonal antibodies were detected using anti rabbit IgG, an horseradish peroxidase (HRP)-linked heavy and light chain antibody from goat (A120-101P, Bethyl Laboratories, Montgomery, TX, USA); mouse monoclonal antibodies were detected using anti-mouse IgG, an HRP-linked heavy and light chain antibody from goat (A90-116P, Bethyl Laboratories). Signals were detected using the enhanced chemiluminescence method (Pierce).

Statistical analyses

Analyses of 'inner' and 'outer' (whole) area of EBs, flow cytometry data, incidence of EB formation and cell number data are all presented as average ± standard deviation (SD). All comparisons between groups were calculated using Student's *t*-test (unpaired, two-tailed) with *P*-values ≤ 0.05 indicating statistical significance.

SUPPLEMENTARY MATERIAL

Supplementary Material is available at *HMG* online.

Conflict of Interest statement. None declared.

FUNDING

Research in our laboratory is supported by the Österreichische Nationalbank.

REFERENCES

1. Prusa, A.R., Marton, E., Rosner, M., Bernaschek, G. and Hengstschläger, M. (2003) Oct4 expressing cells in human amniotic fluid: a new source for stem cell research? *Hum. Reprod.*, **18**, 1489–1493.
2. Aboushwareb, T. and Atala, A. (2008) Stem cells in urology. *Nat. Clin. Pract. Urol.*, **5**, 621–631.
3. Rosner, M., Mikula, M., Preitschopf, A., Feichtinger, M., Schipany, K. and Hengstschläger, M. (2011) Neurogenic differentiation of amniotic fluid stem cells. *Amino Acids*, doi 10.1007/s00726-011-0929-8.
4. De Coppi, P., Bartsch, G., Siddiqui, M.M., Xu, T., Santos, T.X., Perin, L., Mostoslavsky, G., Serre, A.C., Snyder, E.Y., Yoo, J.J. *et al.* (2007) Isolation of amniotic stem cell lines with potential for therapy. *Nat. Biotechnol.*, **25**, 100–106.
5. Siegel, N., Rosner, M., Unbekandt, M., Fuchs, C., Slabina, N., Dolznig, H., Davies, J.A., Lubec, G. and Hengstschläger, M. (2010) Contribution of human amniotic fluid stem cells to renal tissue formation depends on mTOR. *Hum. Mol. Genet.*, **19**, 3320–3331.
6. Koike, M., Sakaki, S., Amano, Y. and Kurosawa, H. (2007) Characterization of embryoid bodies of mouse embryonic stem cells formed under various culture conditions and estimation of differentiation status of such bodies. *J. Biosci. Bioeng.*, **104**, 294–299.
7. Ungrin, M.D., Joshi, C., Nica, A., Bauwens, C. and Zandstra, P.W. (2008) Reproducible, ultra high-troughput formation of multicellular organization from single cell suspension-derived human embryonic stem cell aggregates. *PLoS ONE*, **3**, e1565.
8. Valli, A., Rosner, M., Fuchs, C., Siegel, N., Bishop, C.E., Dolznig, H., Mädel, U., Feichtinger, W., Atala, A. and Hengstschläger, M. (2010) Embryoid body formation of human amniotic fluid stem cells depends on mTOR. *Oncogene*, **29**, 966–977.
9. Rosner, M., Siegel, N., Fuchs, C., Slabina, N., Dolznig, H. and Hengstschläger, M. (2010) Efficient siRNA-mediated prolonged gene silencing in human amniotic fluid stem cells. *Nat. Protoc.*, **5**, 1081–1095.
10. Yang, Q. and Guan, K.-L. (2007) Expanding mTOR signaling. *Cell Res.*, **17**, 666–681.
11. Wang, X. and Proud, C.G. (2009) Nutrient control of TORC1, a cell-cycle regulator. *Trends Cell Biol.*, **19**, 260–267.
12. Sengupta, S., Peterson, T.R. and Sabatini, D.M. (2010) Regulation of the mTOR complex 1 pathway by nutrients, growth factors, and stress. *Mol. Cell*, **40**, 310–322.
13. Freilinger, A., Rosner, M., Krupitza, G., Nishino, M., Lubec, G., Korsmeyer, S.J. and Hengstschläger, M. (2006) Tuberin activates the proapoptotic molecule BAD. *Oncogene*, **25**, 6467–6479.
14. Grusch, M., Polgar, D., Gfatter, S., Leuhuber, K., Huettenbrenner, S., Leisser, C., Fuhrmann, G., Kassie, F., Steinkellner, H., Smid, K. *et al.* (2002) Maintenance of ATP favours apoptosis over necrosis triggered by benzamide riboside. *Cell Death Differ.*, **9**, 169–178.

15. Armstrong, J.F., Pritchard-Jones, K., Bickmore, W.A., Hastie, N.D. and Bard, J.B. (1993) The expression of the Wilms' tumour gene, WT1, in the developing mammalian embryo. *Mech. Dev.*, **40**, 85–97.
16. Cai, J., Chen, J., Liu, Y., Miura, T., Luo, Y., Loring, J.F., Freed, W.J., Rao, M.S. and Zeng, X. (2006) Assessing self-renewal and differentiation in human embryonic stem cell lines. *Stem. Cells*, **24**, 516–530.
17. Ren, X.W., Liang, M., Meng, X., Ye, X., Ma, H., Zhao, Y., Guo, J., Cai, N., Chen, H.Z., Ye, S.L. and Hu, F. (2006) A tumor-specific conditionally replicative adenovirus vector expressing TRAIL for gene therapy of hepatocellular carcinoma. *Cancer Gene Ther.*, **13**, 159–168.
18. Ogden, S.K., Lee, K.C., Wernke-Dollries, K., Stratton, S.A., Aronow, B. and Barton, MC. (2001) p53 targets chromatin structure alteration to repress alpha-fetoprotein gene expression. *J. Biol. Chem.*, **276**, 42057–42062.
19. Mahller, Y.Y., Williams, J.P., Baird, W.H., Mitton, B., Grossheim, J., Saeki, Y., Cancelas, J.A., Ratner, N. and Cripe, T.P. (2009) Neuroblastoma cell lines contain pluripotent tumor initiating cells that are susceptible to a targeted oncolytic virus. *PLoS ONE*, **4**, e4235.
20. Loeb, D.M., Evron, E., Patel, C.B., Sharma, P.M., Niranjan, B., Buluwela, L., Weitzman, S.A., Korz, D. and Sukumar, S. (2001) Wilms' tumor suppressor gene (WT1) is expressed in primary breast tumors despite tumor-specific promoter methylation. *Cancer Res.*, **61**, 921–925.
21. Unbekandt, M. and Davies, J.A. (2010) Dissociation of embryonic kidneys followed by reaggregation allows the formation of renal tissues. *Kidney Int.*, **77**, 407–416.
22. Rosner, M., Freilinger, A., Hanneder, M., Fujita, N., Lubec, G., Tsuruo, T. and Hengstschläger, M. (2007) p27Kip1 localization depends on the tumor suppressor protein tuberin. *Hum. Mol. Genet.*, **16**, 1541–1556.
23. Neuman, N.A. and Henske, E.P. (2011) Non-canonical functions of the tuberous sclerosis complex-Rheb signalling axis. *EMBO Mol. Med.*, **3**, 1–12.
24. Sancak, Y., Thoreen, C.C., Peterson, T.R., Lindquist, R.A., Kang, S.A., Spooner, E., Carr, S.A. and Sabatini, D.M. (2007) PRAS40 is an insulin-regulated inhibitor of the mTORC1 protein kinase. *Mol. Cell*, **25**, 903–915.
25. Wang, L., Harris, T.E., Roth, R.A. and Lawrence, J.C. Jr. (2007) PRAS40 regulates mTORC1 kinase activity by functioning as a direct inhibitor of substrate binding. *J. Biol. Chem.*, **282**, 20036–20044.
26. Thedieck, K., Polak, P., Kim, M.L., Molle, K.D., Cohen, A., Jenö, P., Arrieumerlou, C. and Hall, M.N. (2007) PRAS40 and PRR5-like protein are new mTOR interactors that regulate apoptosis. *PLoS ONE*, **2**, e1217.
27. Fonseca, B.D., Smith, E.M., Lee, V.H., MacKintosh, C. and Proud, C.G. (2007) PRAS40 is a target for mammalian target of rapamycin complex 1 and is required for signaling downstream of this complex. *J. Biol. Chem.*, **282**, 24514–24524.
28. Oshiro, N., Takahashi, R., Yoshino, K., Tanimura, K., Nakashima, A., Eguchi, S., Miyamoto, T., Hara, K., Takehana, K., Avruch, J., Kikkawa, U. and Yonezawa, K. (2007) The proline-rich Akt substrate of 40 kDa (PRAS40) is a physiological substrate of mammalian target of rapamycin complex 1. *J. Biol. Chem.*, **282**, 20329–20339.
29. Choo, A.Y., Yoon, S.O., Kim, S.G., Roux, P.P. and Blenis, J. (2008) Rapamycin differently inhibits S6Ks and 4E-BP1 to mediate cell type-specific repression of mRNA translation. *Proc. Natl Acad. Sci. USA*, **105**, 17414–17419.
30. Sarbassov, D.D., Ali, S.M., Sengupta, S., Sheen, J.H., Hsu, P.P., Bagley, A.F., Markhard, A.L. and Sabatini, D.M. (2006) Prolonged rapamycin treatment inhibits mTORC2 assembly and Akt/PKB. *Mol. Cell*, **22**, 159–168.
31. Rosner, M. and Hengstschläger, M. (2008) Cytoplasmic and nuclear distribution of the protein complex mTORC1 and mTORC2: rapamycin triggers dephosphorylation and delocalization of the mTORC2 components rictor and sin1. *Hum. Mol. Genet.*, **17**, 2934–2948.
32. Zhou, J., Su, P., Wang, L., Chen, J., Zimmermann, M., Genbacev, O., Afonja, O., Horne, M.C., Tanaka, T., Duan, E. *et al.* (2009) mTOR supports long-term self-renewal and suppresses mesoderm and endoderm activites of human ambryonic stem cells. *Proc. Natl Acad. Sci. USA*, **106**, 7840–7845.
33. Rosner, M., Hanneder, M., Siegel, N., Valli, A., Fuchs, C. and Hengstschläger, M. (2008) The mTOR pathway and its role in human genetic diseases. *Mutat. Res. Rev. Mutat. Res.*, **659**, 284–292.
34. Nascimento, E.B.M. and Ouwens, D.M. (2009) PRAS40: Target or modulator of mTORC1 signalling and insulin action? *Arch. Physiol. Biochem.*, **115**, 163–175.
35. Onda, H., Lueck, A., Marks, P.W., Warren, H.B. and Kwiatkowski, D.J. (1999) Tsc2(+/-) mice develop tumors in multiple sites that express gelsolin and are influenced by genetic background. *J. Clin. Invest.*, **104**, 687–695.
36. Kobayashi, T., Minowa, O., Kuno, J., Mitani, H., Hino, O. and Noda, T. (1999) Renal carcinogenesis, hepatic hemangiomatosis, and embryonic lethality caused by a germ-line Tsc2 mutation in mice. *Cancer Res.*, **59**, 1206–1211.
37. Gangloff, Y.G., Mueller, M., Dann, S.G., Svoboda, P., Sticker, M., Spetz, J.F., Um, S.H., Brown, E.J., Cereghini, S., Thomas, G. and Kozma, S.C. (2004) Disruption of the mouse mTOR gene leads to early postimplantation lethality and prohibits embryonic stem cell development. *Mol. Cell Biol.*, **24**, 9508–9516.
38. Murakami, M., Ichisaka, T., Maeda, M., Oshiro, N., Hara, K., Edenhofer, F., Kiyama, H., Yonezawa, K. and Yamanaka, S. (2004) mTOR is essential for growth and proliferation in early mouse embryos and embryonic stem cells. *Mol. Cell Biol.*, **24**, 6710–6718.
39. Hentges, K.E., Sirry, B., Gingeras, A.C., Sarbassov, D., Sonenberg, N., Sabatini, D. and Peterson, A.S. (2001) FRAP/mTOR is required for proliferation and patterning during embryonic development in the mouse. *Proc. Natl Acad. Sci. USA*, **98**, 13796–13801.
40. Jirmanova, L., Afanassieff, M., Gobert-Gosse, S., Markossian, S. and Savatier, P. (2002) Differential contributions of ERK and PI3-kinase to the regulation of cyclin D1 expression and to the control of the G1/S transition in moue embryonic stem cells. *Oncogene*, **21**, 5515–5528.
41. Kawasome, H., Papst, P., Webb, S., Keller, G.M., Johnson, G.L., Gelfand, E.W. and Terada, N. (1998) Targeted disruption of p70(S6K) defines its role in protein synthesis and rapamycin sensitivity. *Proc. Natl Acad. Sci. USA*, **95**, 5033–5038.
42. Madhunapantula, S.V., Sharma, A. and Robertson, G.P. (2007) PRAS40 deregulates apoptosis in malignant melanoma. *Cancer Res.*, **67**, 3626–3636.
43. Inoki, K., Zhu, T. and Guan, K-L. (2003) TSC2 mediates cellular energy response to control cell growth and survival. *Cell*, **115**, 577–590.
44. Freilinger, A., Rosner, M., Hanneder, M. and Hengstschläger, M. (2008) Ras mediates cell survival by regulating tuberin. *Oncogene*, **27**, 2072–2083.
45. Ghosh, S., Tergaonkar, V., Rothlin, C.V., Correa, R.G., Bottero, V., Bist, P., Verma, I.M. and Hunter, T. (2006) Essential role of tuberous sclerosis genes TSC1 and TSC2 in NF-kappaB activation and cell survival. *Cancer Cell*, **10**, 215–226.
46. Kang, Y.J., Lu, M.K. and Guan, K-L. (2011) The TSC1 and TSC2 tumor suppressors are required for proper ER stress response and protect cells from ER stress-induced apoptosis. *Cell Death Differ.*, **18**, 133–144.
47. Thoreen, C.C., Kang, S.A., Chang, J.W., Liu, Q., Zhang, J., Gao, Y., Reichling, L.J., Sim, T., Sabatini, D.M. and Gray, N.S. (2009) An ATP-competitive mammalian target of rapamycin inhibitor reveals rapamycin-resistant functions of mTORC1. *J. Biol. Chem.*, **284**, 8023–8032.
48. Rosner, M., Hofer, K., Kubista, M. and Hengstschläger, M. (2003) Cell size regulation by the human TSC tumor suppressor proteins depends on PI3K and FKBP38. *Oncogene*, **22**, 4786–4798.